TWO-DIMENSIONAL CFD-BASED PARAMETRIC ANALYSIS OF DOWNWIND SAIL DESIGNS

S. J. Collie , University of Auckland, NZ, **P. S. Jackson**, University of Auckland, NZ, **M. Gerritsen**, Stanford University, USA, and **J.B. Fallow**, North Sails New Zealand Ltd., NZ

SUMMARY

This paper presents results from a Computational Fluid Dynamics (CFD) based parametric design study of two-dimensional downwind sail sections. By varying draft and camber a range of sail shapes are generated that cover the typical range of an America's Cup Class (ACC) downwind sail inventory. In order to reduce simulation times only a solitary downwind sail is used, i.e., the influence of the mainsail is ignored. One series of simulations is also carried out with a mainsail included to establish the impact of the mainsail's presence and to determine whether or not downwind sails can be designed - in two-dimensions at least - whilst ignoring the influence of the mainsail. Results show that very high lift coefficients (2.1-2.5) can be obtained for two-dimensional downwind sail sections. These lift coefficients are considerably higher than lift coefficient values (1.0-1.7) typically used in Velocity Prediction Programs (VPPs) indicating that real downwind sails experience three-dimensional effects that hinder their performance considerably.

Nomenclature

α	Angle of attack ($^\circ$)
Γ	Circulation ($m^2.s^{-1}$)
ν	Kinematic viscosity ($m^2.s^{-1}$)
ρ	Density ($kg.m^{-3}$)
ω	Specific rate of dissipation of turbulent kinetic energy (s^{-1})
c	Chord length (m)
C_L	Lift coefficient
$C_{L(\max)}$	Maximum lift coefficient
C_P	Pressure Coefficient
k	Turbulent kinetic energy ($m^2.s^{-2}$)
τ_w	Wall shear stress ($kg.s^{-2}.m^{-1}$)
u_τ	Friction velocity ($u_\tau = (\tau_w/\rho)^{1/2}$) ($m.s^{-1}$)
y	Distance to the nearerst wall boundary (m)
y^+	Non-dimensional wall distance ($y^+ = \frac{u_\tau y}{\nu}$)

ACC	Americas Cup Class
CFD	Computational Fluid Dynamics
PC	Personal Computer
SST	Shear Stress Transport
VPP	Velocity Prediction Program

1 Introduction

With the rapid advancement and depreciating cost of high-end computers, engineers and designers are increasingly tempted to invest in computational methods. However, unlike many other aspects of yacht and sail design, downwind sail development is yet to make use of Computational Fluid Dynamics (CFD) tools. The flow field around downwind sails is complex and involves extensive regions of separated flow. Consequently, the downwind sail design process is largely empirical, based around incremental developments and experiences with past designs. Recently wind tunnel testing has become an integral part of high performance downwind sail development and with the current rate of increase of CFD technology and computer power the inclusion of CFD in the design process is inevitable.

In contrast to downwind sails, it is common for sail designers to rely almost entirely on computational approaches in the design of upwind sails. Upwind sails have low camber and operate at efficient lift-to-drag ratios in a similar fashion to airfoils designed for cruise conditions. Unfortunately, wind tunnel tests are less accurate for upwind studies due to difficulties in producing a realistic onset flow and in trimming the sails accurately. Panel methods such as the vortex-lattice method [1, 2] are well established for use in the computation of upwind sail flows. Such codes can provide three-dimensional solutions for the flow past genoa/mainsail configurations in less than a minute on a common desktop PC. Consequently extensive parametric design studies can be carried out using a large number of design variables. However, panel methods are only valid for close-hauled sailing conditions where the flow remains attached. In fact, their inability to predict leading edge and trailing edge separation makes the application of panel methods for performance prediction questionable even in close-hauled conditions. Consequently they are seldom relied upon for aerodynamic input into velocity prediction programs (VPPs).

When sailing downwind ACC yachts experience an apparent wind direction that can be anything from 50° to 150°. In average conditions the apparent wind angle is usually around 90° and consequently the lift force is the primary contributor to the driving force of the yacht and the drag force has more influence on the

yachts heeling moment and heeling force. Unlike when sailing upwind, the heeling force on a yacht travelling downwind has little influence on performance since the loads on the keel are far less and the yacht heels only slightly. Therefore downwind sails are generally designed and trimmed in order to maximise lift while paying little consideration to drag. Even when sailing at deep angles where the drag contributes to driving force (i.e. above 90°), the increase in drag that is experienced at angles above the maximum lift angle (i.e. post stall) does not successfully compensate for the loss of lift due to stall. Consequently downwind sails are nearly always trimmed to maximise lift and therefore they are sheeted to similar angles of attack relative to the chord line across a wide range of apparent wind angles.

There are several clear advantages of CFD over wind tunnel testing for downwind sail design. Wind tunnel testing is plagued by inaccuracies in the model construction and in obtaining the correct sail trim. In a CFD simulation the geometry is fixed and can be taken either from digitized photographic data, or from an aeroelastic analysis. Furthermore, since wind tunnel models are much smaller than real sails, scaling errors are introduced, both in terms of the inviscid/viscid behavior (Reynolds number) and in the deformation of the model under load (strain scaling). Difficulties are also found in creating realistic flow conditions since the problem is complicated by the twisted apparent wind profile that is created as the yacht travels within the atmospheric boundary layer. At present only three wind tunnels in the world are known to have the facility to reproduce twisted flow for sailing yachts; the twisted flow wind tunnel (TFWT) [3] at The University of Auckland's Yacht Research Unit and similar tunnels in California and Italy commissioned by Oracle BMW racing and Prada respectively.

The computational demands for a CFD model of a three-dimensional sail are considerable. Grid accurate analysis requires computational grids in excess of 10 million nodes and consequently many gigabytes of computer memory are required. Due to the unsteady nature of downwind sail flows the simulations must use a transient solver and time steps small enough to resolve the transient behavior. Even with state-of-the-art supercomputers, simulations of this flow problem inevitably take days, or even weeks, to solve. Considering the computational demands of a single simulation of the flow past a downwind sail configuration, performing a comprehensive design study with suitable grid- and time-step convergence studies for a three-dimensional model would require exorbitant computer resources.

This study focuses on flows around two-dimensional downwind sail sections and serves as an initial examination of the downwind design space, with a goal to obtain an indication of the maximum lift coefficient that can be generated from a single thin-membrane airfoil. The prospect of using CFD for parametric analysis of the three-dimensional downwind design space is daunting and remains as yet untackled. Several CFD studies [4, 5] have investigated the three-dimensional flow around downwind sails, however these studies did not capture the transient nature of the flow. Whilst it is acknowledged that the current work does not directly relate to three-dimensional sail designs, the study does still provide an indication of the influence of draft and camber on downwind sail performance. The current work is part of a larger research project which is believed to be the first significant CFD investigation into the unsteady two-dimensional flow around downwind sail designs.

1.1 Description of the flow structure

When sailing downwind the sails are designed to maximise the driving force. Aerodynamic lift is the primary contributor to this force and little attention is paid to reducing the drag (in fact drag often contributes to driving force). Consequently downwind sails typically have a large amount of camber (20-30%) and operate at high angles of attack (25-35 degrees to the chord line of the sail) and as a result there is extensive trailing edge separation. A two-dimensional schematic of the flow past a section from a downwind sail near mid height is illustrated in Figure 1. In order to support the sail - which is a flexible membrane - the forward stagnation point must rest on the windward (pressure) side of the sail just back from the leading edge (luff). If the flow stagnates on the leeward (suction) surface of the sail then the luff of the sail will collapse (for non-rigid sails) due to the pressure difference across the sail. When real sails are trimmed they are initially sheeted out (i.e. the sheets are let out to lower the angle of attack) until the luff of the sail begins to collapse and then the sail is sheeted in slightly until the luff resets. In this fashion the sails are set to the lowest possible angle where the sail remains inflated and stable.

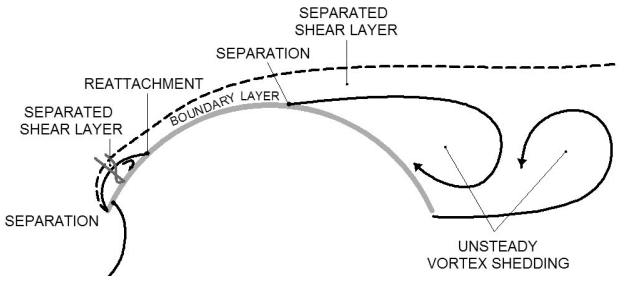

Figure 1: A two-dimensional downwind sail flow.

A particularly interesting feature of sail flows is the

existence of a short leading edge bubble on the leeward surface of the sail. This bubble is formed as the flow separates as it attempts to round the sharp leading edge. The leading edge bubble typically reattaches within the first 10% of the chord length, c, and downstream of reattachment a turbulent boundary layer develops. Trailing edge separation generally occurs soon after the position of maximum thickness (the draft position) due to an adverse pressure gradient that typically extends across the rear half of the sail.

The trailing edge separation region is unsteady and periodic with counter rotating vortices being shed alternately from the windward and leeward surfaces of the sail. This unsteady process has a considerable effect on the loading of the sail with the forces oscillating in a sinusoidal fashion. Since the circulation, Γ, of the sail is changing the angle of incidence to the leading edge also oscillates, hence the positions of stagnation, reattachment and separation points must also vary in a periodic manner.

2 The Approach

2.1 The sail sections

Figure 2 illustrates the method for defining sail sections that is used by North Sails New Zealand Limited. The shapes are described by the draft, camber, front percentage, back percentage, leading edge angle and trailing edge angle. These parameters are illustrated in Figure 2 and defined as follows:

- **Camber** = $\frac{y_{\max}}{c}$, where $y_{\max}$ is the greatest perpendicular distance between the sail and the chord line.
- **Draft** = $\frac{x_d}{c}$, where x_d is the chordwise location of $y_{\max}$.
- **Front percentage** = $\frac{y_{front}}{y_{\max}}$, where y_{front} is the perpendicular distance between the sail and the chord line halfway between the leading edge and x_d.
- **Back percentage** = $\frac{y_{back}}{y_{\max}}$, where y_{back} is the perpendicular distance between the sail and the chord line halfway between x_d and the trailing edge.
- **Leading edge angle** is the slope of the tangent to the sail at the leading edge.
- **Trailing edge angle** is the slope of the tangent to the sail at the trailing edge.

Using these parameters our sail shapes are generated using two fourth-order Bezier curves. The two curves

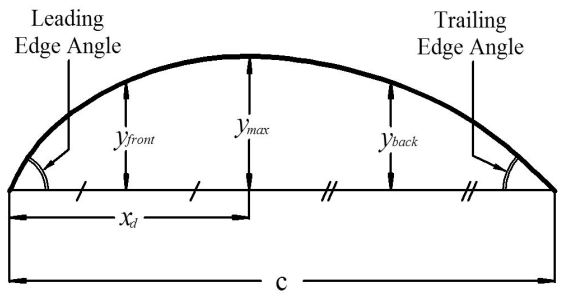

Figure 2: A sail section with its defining geometry.

meet at the maximum draft position $(x_d, y_{\max})$, and at this point the sail's curvature and the first derivative of curvature are forced to be continuous.

Six different camber values were tested: 21%, 23%, 25%, 27%, 29% and 31%. For each camber the draft was set at 40%, 45%, 50% and 55% which in total gave 24 different section shapes. The design with 23% camber and 45% draft was based upon a horizontal slice from the flying shape of one of Team New Zealand's mid-range gennakers. The sail shapes are identified using the naming convention XXYY, where XX is the camber and YY is the draft, i.e., section 2345 has 23% camber and 45% draft.

For all sails tested in this study the leading and trailing edge angles were fixed at 60 and 50 degrees respectively, and the front and back percentages were set at 82.45% and 79.87% respectively, which were the values from the base design. Leading and trailing edge angle as well as front and back percentage are parameters which certainly influence the performance of downwind sails and ideally these parameters should be included in any parametric studies. However in order to reduce the number of simulations required in this study a decision was made to limit the design variables to the three parameters that have the most influence on the design, namely camber, draft and angle of attack.

2.2 Performance analysis

For the current study the force coefficients were measured at four different angles of attack around the angle of maximum lift. The CFD results computed in this study suggest that the sail sections experience maximum lift at an angle of attack of 18.5° ±3° and accordingly the forces were evaluated at α =15°, 17.5°, 20° and 22.5°. The forces were then fitted with a cubic polynomial and the lift coefficients at maximum lift were determined from this fit. In order to evaluate the accuracy of this method simulations were performed at several other angles of attack for the

base design (section 2345). The results of this investigation are presented in Section 3.1.

2.3 The CFD model

The software used in this study is CFX-5, an unstructured commercial CFD package. In the CFX-5 solver the RANS equations are discretised using a conservative and time-implicit finite volume method and solved using an additive correction algebraic multigrid (AMG) solver accelerated with an incomplete upper lower (ILU) factorisation technique. Details of these techniques and their implementation can be found in [6] and [7]. Spatial interpolation is carried out using a bounded high-resolution advection scheme, details of which can be found in [6] and [8]. Time integration was carried out using second-order backward Euler time-stepping and a series of 4 inner-iterations within each time-step to update the non-linear coefficients.

Turbulence is modelled using the SST $k-\omega$ turbulence model [9] which has stood out in recent years as the most suitable model for high-lift aerodynamic applications [10]. Validation studies carried out by the authors for highly cambered sail sections have indicated that the SST model is indeed the most suitable turbulence model in CFX-5 for computing the flow past downwind sails [11].

The sail sections were modelled as infinitely thin walls with no-slip boundary conditions. At the inlet Cartesian velocity components are specified according to the angle of incidence. For all simulations the chord length, c, was set at $1m$ and the Reynolds number based on chord length was set at approximately 3.31×10^6. For a typical downwind sail (chord length $\simeq 14m$ at mid girth) this Reynolds number corresponds to apparent wind speed of approximately $3.5m.s^{-1}$ or 7 knots which is a typical apparent wind speed for an ACC yacht. At the inlet the freestream turbulence intensity was set at 1% with a length scale of $0.001m$, however the CFD solutions were independent of these values. At the outlet a zero static pressure boundary condition was imposed.

The computational grids used in this study are all structured curvilinear grids generated in ICEM-HEXA [12]. A grid convergence study was conducted for the 2345 section using three grids that are referred to as coarse, medium and fine with 13200, 55380 and 225940 cells respectively. As the grid was refined convergence of the lift and drag coefficients was evident indicating satisfactory grid independence. The medium grid (see Figure 3) was therefore chosen as the most suitable grid for the study. In order to achieve a y^+ of approximately 1.0 the near wall spacing was set at $6.25 \times 10^{-5}c$. Particular care was taken to provide high quality cells around the leading and trailing edges and in these regions the cells have an aspect ratio of $1:1$. The leading edge region is illustrated in the close-up view in Figure 3. Further along the sail, very high aspect ratio cells are used in order to resolve the large flow gradients normal to the wall.

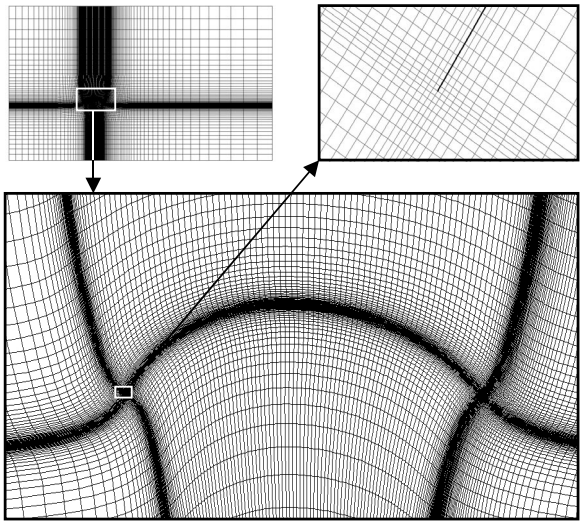

Figure 3: The medium grid from the grid convergence study.

Initial simulations indicated that timesteps as low as $0.00125s$ were required in order to adequately capture the transient behavior. Time step convergence was investigated by starting with a time step of $0.00125s$ and then repeating the simulations with the time step halved and then halved again, i.e. the time step sizes used are $0.00125s$, $0.000625s$ and $0.0003125s$. As the timestep size is reduced both the lift and drag coefficients level off indicating satisfactory time-step convergence. The lift for the solution using the medium time step is within 0.075% of the lift computed using the short time step and the drag is within 0.19%. The medium time step size corresponds to approximately 33 time steps per shedding cycle for the $\alpha = 15^\circ$ case and 54 time steps per shedding cycle for the $\alpha = 22.5^\circ$ case. In all cases in this paper the force coefficient values presented are the time-averaged values. That is, the simulations are run until they are converged to a periodic steady state and the forces are then averaged over the final shedding cycle.

3 Results

3.1 Performance of the base sail section

The time-averaged lift coefficient versus angle of attack for the 2345 section is plotted in Figure 4. Also plotted is a polynomial fit through the data points at 15°, 17.5°, 20° and 22.5° (highlighted). The fitted curve estimates the maximum lift coefficient to be 2.26 and to occur at 19.8°. As can be seen in Figure

4b the fitted curve agrees well with the data points at 18.75° and 21.25° and therefore it should also provide a suitable prediction for $C_{L\max}$. The drag coefficient at maximum lift for this sail section is 0.34 and the lift-to-drag ratio is 6.65.

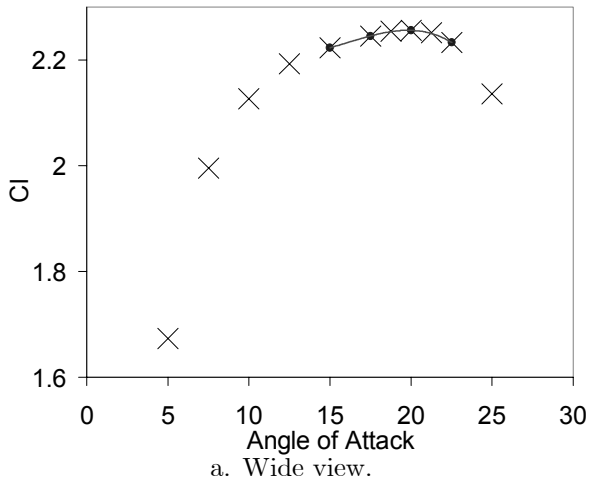

a. Wide view.

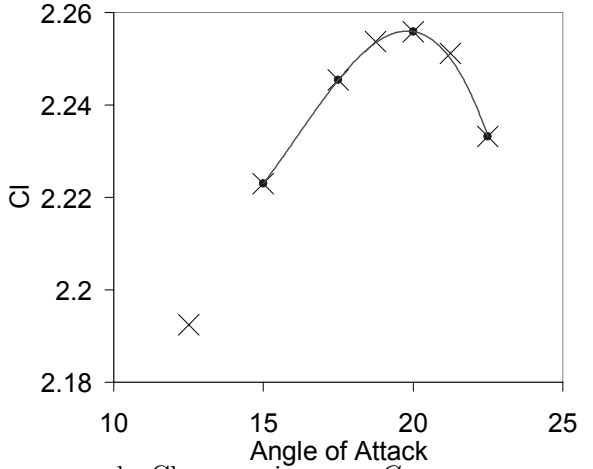

b. Close up view near $C_{L\max}$.

Figure 4: Lift versus angle of attack for the 2345 section.

3.2 Mainsail influence

Mainsail/headsail interaction is a well covered and debated subject in upwind sail design (see [13, 14]), however little work has gone into such interactions for downwind sailing. Wind tunnel experiments have been carried out at the University of Auckland's Yacht Research Unit investigating gennaker/mainsail interaction by measuring the sail forces independently [15, 16]. Results showed that, when tested both in isolation and together, the total lift of the gennaker/mainsail configuration was less than the sum of its parts. Results also showed that the forces on the mainsail were adversely influenced by the presence of the gennaker. However, nothing conclusive could be said about the influence of the mainsail on the gennaker, it was difficult to distinguish between the lift and drag forces measured on the gennaker with and without the mainsail present. Richards et al. [17] suggest that since the forces on the gennaker are not significantly affected by the presence of the mainsail "it is possible to consider their optimisation independently". However, this assumption does not consider the effect that the mainsail has on the flow over the gennaker and the fact that it is possible for two different flows to produce the same force coefficients. Therefore there is not sufficient evidence to say that gennakers can be appropriately designed and tested in isolation since the mainsail still may well have significant influence on the flow field of the gennaker even if this interaction has little influence on the forces.

In the present study the flow past the 2345 gennaker is modeled in conjunction with a mainsail with shape and position determined using overhead photography of a wind tunnel model for an apparent wind direction of 90°. The geometry corresponds to a two-dimensional slice taken approximately midway up the mainsail. The grid used in this study is based upon the single sail grid (Figure 3). The grid has 130685 cells, which is considerably more than the single sail grid since it must also capture the boundary layer and wake of the mainsail. Initial simulations showed that the mainsail was considerably stalled compared with the flow visualised in three-dimensional wind tunnel tests and to alleviate this problem the mainsail was rotated anti-clockwise by 10° which produced a more realistic flow pattern. This discrepancy between the two- and three -dimensional configurations is due to three-dimensional downwash which effectively lowers the angle of attack to the mainsail in the three-dimensional configuration.

Figure 5 presents a comparison between the flow field for the gennaker/mainsail configuration (Figure 5a) and the flow field for the solitary gennaker (Figure 5b). The main difference that can be seen for gennaker/mainsail configuration is that streamlines have more upwards curvature upstream of the gennaker (Figure 5a), an interaction that has been well documented (see [13, 14]). The effect is partially due to the circulation from the mainsail providing upwash, however the effect of the slot between the two sails has a more pronounced contribution. Within the slot the individual circulation fields around the gennaker and mainsail oppose each other and the flow is not significantly accelerated by the venturi-like contraction that the slot creates (although the balance of circulation fields of the two sails may well accelerate the flow within the slot). Instead much of the flow upstream of the slot is diverted around the sails, i.e. to leeward of the gennaker and to windward of the mainsail. Consequently the luff of the gennaker sees a higher angle of attack than it would if the mainsail was not present

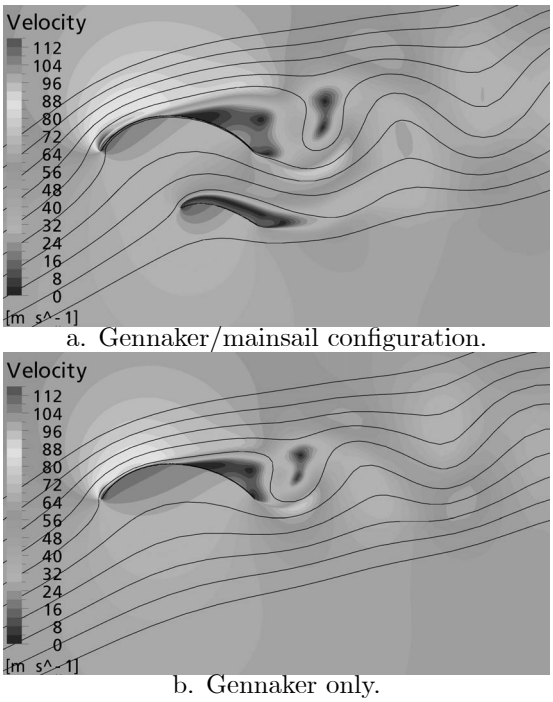

a. Gennaker/mainsail configuration.

b. Gennaker only.

Figure 5: Comparison of the flow streamlines and velocity contours for the gennaker / mainsail conguration (a) and the gennaker without the mainsail present (b) ($\alpha = 20°$). The simulations are unsteady and the plots presented are at the same phase angle (180 degrees).

and the mainsail sees a lower angle of attack than it would if the gennaker was not present.

The increased angle of attack upstream of the gennaker leads to a larger leading edge bubble and higher velocities (and hence also more suction) around the leading edge in Figure 5a compared with Figure 5b. It is also noticeable that with the mainsail present the gennaker has a larger trailing edge separation region. These effects can also be seen in the pressure coefficient plot in Figure 6. The gennaker/mainsail configuration has a larger suction peak at the leading edge and the pressure coefficient flattens out (indicating trailing edge separation) earlier than in the simulation without the mainsail.

Whilst the flow upstream of the gennaker is clearly rotated upwards due to the influence of the mainsail, the pressure coefficient plots do not compare well with those for the gennaker in isolation at higher angles of attack. For the single sail simulations if the angle of attack is increased beyond 20 degrees the sail begins to stall. The amount of trailing edge separation increases rapidly until the sail fully separates at approximately 25 degrees. In fact it is impossible to obtain a pressure peak of $C_P = -4$ for the single sail simulation at any angle of attack. For the gennaker/mainsail configuration the mainsail enables

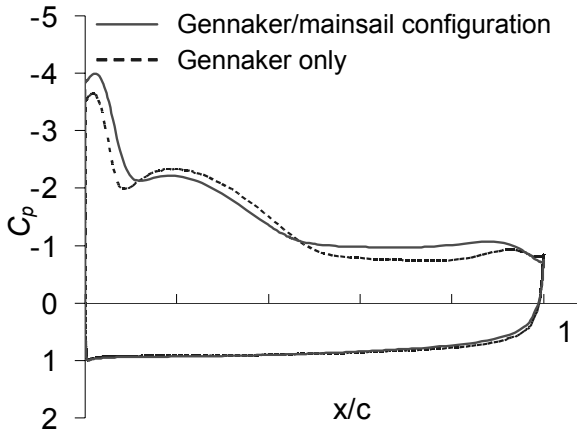

Figure 6: Pressure coefficient plots for the gennaker with and without the mainsail present ($\alpha = 20°$).

the gennaker to sustain a higher suction peak without stalling. This is because the influence of the mainsail is not uniform along the length of the gennaker. Towards the trailing edge of the gennaker the circulation field of the mainsail helps accelerate the flow in the streamwise direction which aids the attached flow on the leeward side of the gennaker and effectively delays separation considering the size of the suction peak. Consequently, higher lift coefficients are obtainable for the gennaker with the mainsail present than without it. For the current study the $C_{L\,\max}$ of the gennaker was 11.9% higher for the gennaker/mainsail configuration than for the gennaker by itself. For the gennaker/mainsail configuration $C_{L\,\max}$ of the gennaker occurs at an angle of attack of 17.12° compared with 19.8° for the gennaker by itself. The lift versus angle of attack curve for the gennaker/mainsail configuration is plotted in Figure 7 along with the lift for the gennaker by itself.

This study illustrates that the mainsail does have significant influence on the flow over the gennaker and that ideally any optimisation of downwind sail shapes should be carried out with the mainsail present. It is likely that the performance ranking of the designs would not be preserved between studies conducted with and without the mainsail present. Nevertheless, for the remainder of the study the downwind sail shapes were tested in isolation since it is felt that initial validation of any design method should be performed in the simplest possible configuration to allow a more rapid exploration of the design space. The study provides a qualitative indication of the influence of draft and camber on downwind sail performance. Also, one of the main purposes of the study was to answer the question of how much lift can potentially be generated by a single thin-membrane airfoil.

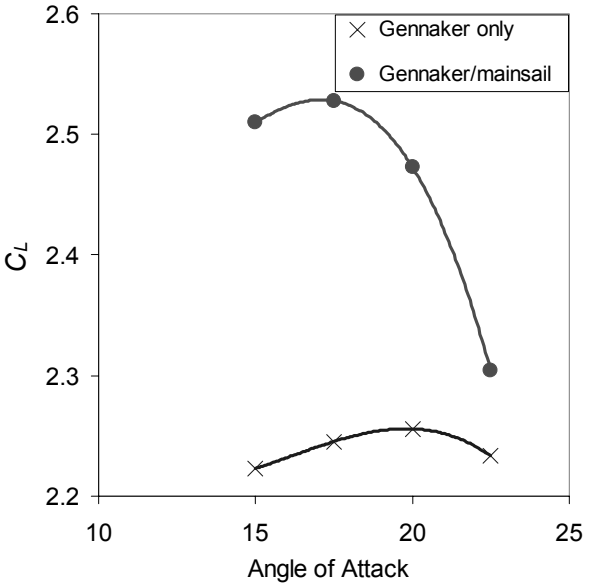

Figure 7: Lift versus angle of attack for the gennaker/mainsail configuration and the gennaker by itself.

3.3 Effects of sail camber

For most airfoils, increasing the camber results in an increase in lift and an associated increase in drag due to steeper pressure recovery (and possibly separation) on the suction side of the foil. Thin airfoil theory predicts that lift will increase linearly with camber at a slope of 2π. However, thin airfoil theory is only valid for small camber values and small angles of attack and downwind sails operate well outside the validity of thin airfoil theory. In this section we look at the relationship between camber and maximum lift at a camber range much higher than where conventional airfoils operate. A plot of maximum lift versus camber for our downwind sail shapes is illustrated in Figure 8. Recall that for each camber four different sails were analysed, each with a different draft percentage. The lift coefficient presented in Figure 8 is an average across the range of draft positions. The chart illustrates that even at these high camber values $C_{L\,\max}$ continues to increase with camber and reaches a maximum at 30.44% camber, above which $C_{L\,\max}$ begins to decrease.

Figure 8 suggests that the optimal camber for a downwind sail should be 30.44% if maximising $C_{L\,\max}$ is the design goal, however 25-26% camber is more typical for up-range America's Cup sails. The reason for this is largely due to the way ACC sails are measured which penalises high camber sails. The sail area is defined as

$$SSA = (SLU + SLE) \times (\frac{SF}{12} + \frac{SMG}{3}),$$

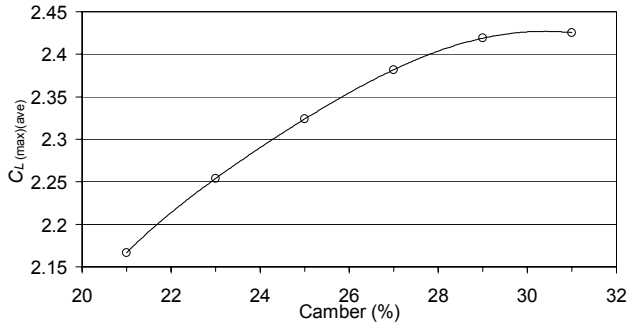

Figure 8: $C_{L\,\max}$ versus camber (where $C_{L\,\max}$ is averaged across the different drafts).

where SSA $[m^2]$ is the measured downwind sail area, SLU is the length of the luff, SLE is the length of the leech, SF is foot length and SMG is the sail's mid girth, defined as the arc length from the mid point of the luff to the mid point of the leech. Both the foot length and the mid girth measurement incorporate camber since it is the actual arc length that is measured at these sections rather than the chord length. Therefore in order to make the current results relevant to America's Cup design the arc length of the sail sections must be used as the length scale in the calculation of the lift coefficient. A plot of the scaled lift versus camber is given in Figure 9, where $C_{LS\,\max}$, the maximum lift coefficient scaled by arc length, s, is now the variable on the y-axis.

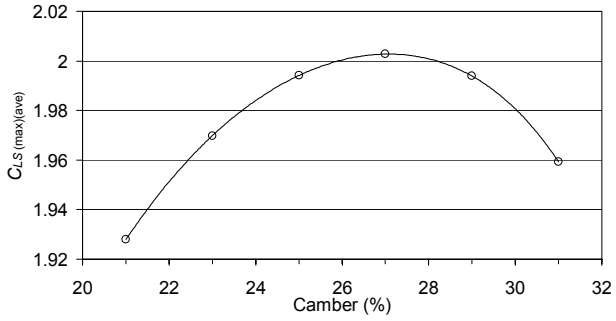

Figure 9: $C_{LS\,\max}$ versus camber (where $C_{LS\,\max}$ is scaled by the arc length and averaged across the different draft values).

From Figure 9 the optimal camber is now 27.03 % which is in much better agreement with America's Cup designs. Typically, up-range downwind sails have 25-26% camber in the mid girth and sails that are designed for light airs may have considerably less camber. Often downwind sails have more camber near the head of the sail since this region is unmeasured and hence it is possible to gain sail area for free. So a sail designer might favour a slightly smaller mid girth camber in order to lower the measured sail area.

Another reason for low camber sails being favoured for America's Cup downwind sails is the effect of induced drag. The most apparent effect of three-dimensional effects is a rotation of the lift-drag axis due to downwash. Consequently drag is increased and lift is decreased relative to the two-dimensional coefficients. Therefore if the heeling force is positive (i.e. the boat is heeling to leeward) then any increase in induced drag is directly diminishing the driving force. This is the typical situation in light to medium wind strengths, or when the yacht is pointing high (i.e. gybing through large angles). In the design of sails for such situations designers look to reduce both induced drag and profile drag by building flat sails with large span. In heavy airs yachts often heel to windward and induced drag rotates the total force closer to the direction the yacht is travelling. Therefore one could make the mistake of assuming that three-dimensional effects are improving the performance of the yacht. It is true that induced drag is less important in heavy airs however three-dimensional effects do still reduce the performance of the sails. The total force coefficient for a three-dimensional sail flow is lower than that achievable in purely two-dimensional flow due to pressure leakage at the tips. Therefore designers are always looking to reduce three-dimensional effects and consequently it is not surprising that America's Cup sails seldom have camber as high as the optimal predicted by this two-dimensional study.

3.4 Effects of sail draft

Despite being more difficult to gybe, asymmetrical sails (gennakers) have often proven to be more effective than symmetrical spinnakers, most noticeably at lower wind strengths. Gennakers were developed primarily to allow the luff to be longer than leech, thus providing more sail area in the forward section of the sail from where most of the lift force is generated (especially at small apparent wind angles). Asymmetrical sails also permit the draft position to be moved away from the middle of the sail (mitre) and it was found that gennakers with the draft forward of 50% were favoured, particularly in light airs. Gennakers are used more and more in the America's Cup and in the 2003 regatta many syndicates used them in winds of 15kts and above, wind strengths where spinnakers had previously been used exclusively.

In this study we look at the influence of the draft position on lift coefficient for our two-dimensional sail sections. Figure 10 presents the results for the scaled maximum lift coefficient, $C_{LS\,\max}$, versus draft, where $C_{LS\,\max}$ is averaged across the six camber values tested. The plot shows the maximum lift coefficient increasing with draft and indicates that the optimal draft position is 54.66%. This result was initially surprising since real sails are always either symmetric (spinnakers) or have the draft forward of 50% (gennakers).

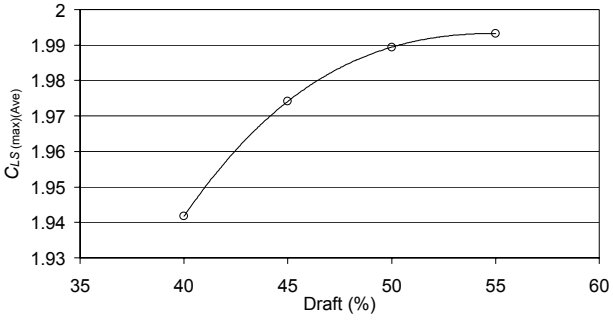

Figure 10: $C_{LS\,\max}$ versus draft (where $C_{LS\,\max}$ is scaled by the arc length and averaged across the different camber values).

Gennakers with the draft position pushed back perform well since they experience less trailing edge separation. Such sails have a longer region downstream of leading edge reattachment where the sail is flat and the boundary layer can recover and build speed. Consequently there is a greater pressure difference across the sail in the area between 30-60% x/c than can be achieved for sails with the draft position further forward. At the high end of the wind range the pole is rotated well to weather and it is this mid region of the sail around the mitre where the majority of the driving force is generated.

The high lift coefficients obtained for sail sections with the draft position at 55% can also be explained through analogy to airfoils with trailing edge flaps. The region near the trailing edge of an airfoil's camber line has the greatest effect on the lift. By increasing the curvature of the camber-line in this region the circulation of the airfoil is increased which causes more upwash upstream of the airfoil, and higher velocities around the leading edge. This means that airfoils with trailing edge flaps are prone to flow separation at the leading edge when the flap is deployed. Consequently such airfoils often have drooped leading edges or leading edge slats that can be drooped as the flap angle is increased. Therefore it is likely that additional improvements in maximum lift could be made by increasing the leading edge angle and the curvature of the sail near the leading edge, thus emulating drooped nose airfoils.

The relationship between draft and performance is also dependent on camber and wind strength. As mentioned, in light airs drag is undesirable and consequently designers favour low camber gennakers with the draft well forward (as low as 40% draft). As the wind strength increases drag becomes less important and camber and draft increase, until at some point spinnakers become favoured due their ease of use and

efficiency though gybes. Therefore it is necessary to look at the relationship between maximum lift and draft over a range of different cambers as is illustrated in Figure 11. From Figure 11 it is evident that it is the higher camber sections that perform better with the draft pushed aft. For the 21% camber sails the optimum draft position predicted by the study is 47.48% whereas for the 31% camber sails the optimum draft position is 60. 09% based upon an extrapolation from Figure 11. Highly cambered sails are more susceptible to early trailing edge separation than low camber sails. As a result it is favourable to push the draft further aft as the camber is increased in order to prevent premature stall.

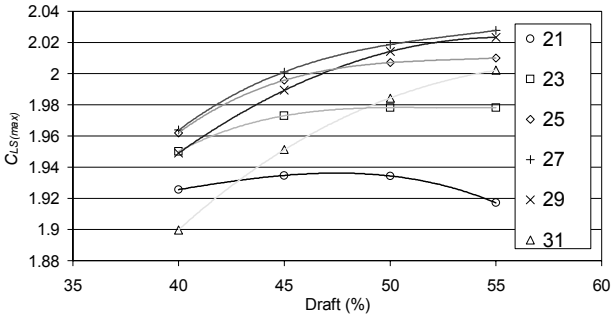

Figure 11: $C_{LS\,\max}$ versus draft for each camber value.

For cambers of 25% and above Figure 11 shows an increase in maximum lift between 50-55% draft suggesting that draft values of 60% and beyond should be included in the study. However increasing the draft further would begin to create sail shapes that are not physically attainable. Sails are supported only at their corners and rely on a positive pressure difference to inflate and therefore the windward surface of the sail must be concave. In this study the trailing edge angle is fixed at 50° and consequently as the draft position moves aft a point of inflection begins to appear near the leech. If we were to look at sails with the draft further aft than 55% then it would be necessary to also increase the trailing edge angle.

In real sail designs the draft is often further forward than the optimal predicted for the lowest camber tested in this study which is due to both three-dimensional effects and the influence of the mainsail. Results from the current study indicate that the trailing edge separation point (at $C_{L\,\max}$) follows the draft position closely with the flow typically separating immediately aft of the draft position. Consequently, by pushing the draft position forward, the separation point also moves forward which can decrease the performance of the sail. For three-dimensional sails, downwash from both three-dimensional effects and the influence of the mainsail diminishes the adverse pressure gradient and the flow is able to remain attached much further aft. Consequently sail designers can get away with pushing the draft position forward whilst keeping the rear separation point well aft. Having the draft position forward is desirable when sailing at small apparent wind angles since it increases the curvature - and hence also the pressure difference - in the region close to the luff. At small apparent wind angles the bulk of the driving force is generated from this region of the sail since the surface normals are closely aligned with the direction the yacht is travelling.

In this study the leading and trailing edge angles were kept constant whereas in reality gennakers that have a draft position well forward will have greater leading edge angles than spinnakers. By leaving the leading edge angle fixed we are limiting the potential increase in curvature around the luff that can be gained by shifting the draft position forward. Perhaps if the leading edge angle had been increased on the sails with the smaller draft values then higher lift coefficients would have been gained for these sails. However, leading edge angle is a design variable in its own right and including leading edge angle in the parametric study would have increased the number of simulations considerably. Whilst any further two-dimensional design studies should investigate leading edge angle (and possibly front and back percentage), it was felt that such as study was unnecessary for this initial exploration of the design space.

This study mimics real trends in sail design with the draft position shifting aft as camber (and wind strength) is increased. However in real sail inventories a choice is generally made to switch to symmetrical spinnakers at wind speeds over a certain strength and consequently sails with the draft position aft of 50% are not used. This study raises the question of whether gennakers with the draft position shifted aft of 50% could provide a performance gain in higher wind strengths and whether symmetrical and draft aft gennakers could eventually replace spinnakers altogether. Several questions remain unanswered. Firstly, will the same trends be witnessed for three-dimensional sails where the stall behavior may be quite different? Also can we even generate a flying shape with maximum draft aft of the mitre? When a sail design comes under load the draft tends to be pushed forward under strain and so designing a shape that will end up flying in the desired shape is not an elementary task. Finally, whilst driving force is the obvious measure of sail performance there are other factors such as the stability of the sail and its ease of trimming and manoeuvring that are also important.

3.5 Driving and heeling force polars

In this section the lift and drag forces on the sails are resolved into driving and heeling force coefficients

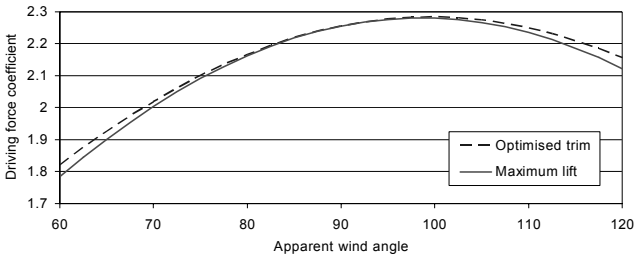

Figure 12: Driving force coefficient for the base section shape (section 2345).

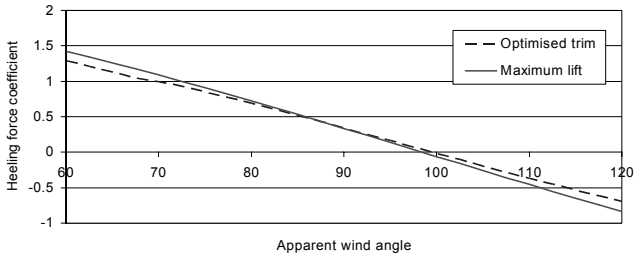

Figure 13: Heeling force coefficient for the base section shape (section 2345).

over a range of apparent wind angles. Since downwind sails are trimmed to maximum lift it is possible to get a good idea of the performance of a particular sail shape through a range of conditions by determining its lift and drag coefficient at maximum lift and resolving the driving and heeling forces across a range of apparent wind angles. This is because changes apparent wind direction result in a solid-body rotation of the sails about the mast. Therefore, the sails shapes remain remarkably constant relative to the apparent wind and one can view the boat as rotating (relative to the apparent wind) underneath the rig. Similarily we can assume that the lift and drag forces on the sail remain constant (reletave to the apparent wind) and it is the driving/heeling force axes that rotate through a change in apparent wind angle.

The driving force coefficient polar for the base sail shape (section 2345) is presented in Figure 12. The plot presents two curves, one for the sail with the angle of attack to the chord line fixed to provide maximum lift, the other with the trim set to maximise the driving force coefficient. The trim optimisation is achieved with a simple conjugate gradient search that adjusts the angle of attack at each apparent wind angle using our polynomial fit for the force coefficients. The greatest difference in driving force coefficient between the two trimming techniques is 1.3% which occurs at the maximum apparent wind angle (120°). At this angle the sail is set at an angle of attack 23.1° for the driving force optimisation. At the lowest apparent wind angle the angle of attack is reduced down to 17.1° for only a 0.5% gain in driving force over the case with the sail trimmed to maximum lift. For this sail shape maximum lift occurs at 19.8°.

The heeling force coefficient polar for the base section shape is presented in Figure 13. Both the optimised and maximum lift trim settings are given and as was found for the driving force both curves are similar with the optimised trim providing only minimal reduction in heeling force. When sailing at small apparent wind angles the heeling force is positive (i.e. the total force points to leeward of the bow) and the boat heels to leeward. At approximately 100° of apparent wind angle the total force points in the same direction as driving force (i.e. all of the aerodynamic force is driving the yacht) and the boat is at zero heel. Above this angle the boat heels to weather. ACC boats have zero heel at around 110 - 120 degrees which is a slightly higher angle than this study suggests. This is due to three-dimensional effects which cause the lift-drag axis to rotate to leeward.

Whilst quite a large range of angles of attack ($17.1° - 23.1°$) was covered in the optimised trim, little gain was made in driving force. This is because our lift polar has a soft stall and there is little change in total force with angle of attack. Real downwind sails are almost always trimmed to maximum lift which suggests that stall is more dramatic and over-trimming the sails (past stall) results in poor boat speed. Similarly under-trimming is undesirable due the inefficiency of having an unstable luff. In three dimensional sail flows downwash effects cause the ideal angle of attack (i.e. the angle where there is no leading edge bubble) to occur at higher angles of attack than in two dimensions. Stall for two-dimensional sails occurs as the rear separation point moves forward and meets the leading edge bubble, this happens slowly resulting in a soft stall pattern. For three-dimensional sail flows there is less trailing edge separation at ideal angle of attack due to downwash induced by three-dimensional effects. However as the angle of attack is increased past ideal angle of attack the leading edge bubble develops and interacts with the tip vortices at the head and foot of the sail. This in turn has a pronounced influence on the downwash distribution over the sail and the trailing edge separation point to moves forward dramatically causing the sail to stall. As a result maximum lift occurs at the ideal angle of attack for real sail flows and the only reason for overtrimming the sails is to keep the luff region stable.

4 Discussion and Conclusions

Downwind sail design is more of an art than it is a science. The evolution of sail designs is largely based upon minor adjustments and refinements to existing

designs with the objective of creating sails that are fast and stable. Unfortunately it is often difficult to determine whether one sail is performing better than another and hence frequently sails are subjectively selected based on appearance. Wind tunnel testing has helped introduce objectivity into the process by providing a means to quantify the performance of different sails. This has revolutionised the way sails are designed and as a consequence many current designs are not the aesthetic creations that have prevailed in the past. This work illustrates how CFD can be utilised in the design cycle, not just for performance prediction but also as a means to obtain better understanding of the flow topology and the behavior of different sail designs.

Despite the loss of direct relevance to real sails due to the omission of the third dimension this two-dimensional study produced interesting results. The relationship between camber and maximum lift follows the same trend as found in three-dimensional sails. The relationship between draft and maximum lift indicates that - for two-dimensions sections at least - there is merit in using sections with the draft values greater than 50% in an effort to delay trailing edge separation for up-range sail designs. Whether this theory will also hold for three-dimensional sails is yet to be determined and any advantages may well be lost due to three-dimensional effects, the influence of the mainsail and issues in constructing and trimming such a sail.

Results from the current study suggest that lift coefficients of the order of $2.4 - 2.5$ are obtainable for two-dimensional downwind sail sections. However the present study imposes limitations on the design space by fixing several of the design variables (front percentage, back percentage, leading edge angle and trailing edge angle) and hence lift coefficients of above 2.5 may very well be possible. Also, downwind sail sections that are aided by the presence of a mainsail can achieve even higher lift coefficients.

Simulations carried out including the mainsail indicate that the mainsail has a pronounced effect on the flow over the gennaker. With the mainsail present the lift on the gennaker was 12% higher than without it. The circulation field of the mainsail has a non-uniform influence on the flow over the gennaker and it is not possible to merely consider the gennaker as seeing an increased angle of attack due to upwash provided by the mainsail. Contribution of the mainsail itself to the yachts driving force cannot be ignored and it is necessary to also consider the influence that the gennaker has on the mainsail. Whilst outside the scope of the current project a two-dimensional investigation of the influence of size of the slot and overlap between the gennaker and mainsail could provide useful results. The relationship between the tip vortices shed from the tips of both sails also needs to be taken into consideration for three-dimensional designs.

References

[1] Katz, J. and Plotkin, A., *Low-Speed Aerodynamics, from Wing Theory to Panel Methods.*, McGraw-Hill Book Co., New York, USA., 1991.

[2] Fiddes, S. and Gaydon, J. H., "A New Vortex Lattice Method for Calculating the Flow Past Yacht Sails," *Journal of Wind Engineering and Industrial Aerodynamics*, Vol. 63, 1996, pp. 35–59.

[3] Flay, R. G. J., "A Twisted Flow Wind Tunnel for Testing Yacht Sails," *Journal of Wind Engineering and Industrial Aerodynamics*, Vol. 63, 1996, pp. 171–182.

[4] Hedges, K. L., Richards, P. J., and Mallinson, G. D., "Computer Modelling of Downwind Sails," *Journal of Wind Engineering and Industrial Aerodynamics*, Vol. 63, 1996, pp. 95–110.

[5] Richter, H. J., Horrigan, K. C., and Braun, J. B., "Computational Fluid Dynamics for Downwind Sails," *The 16th Chesapeake Sailing Yacht Symposium*, 2003, pp. 19–27.

[6] CFX-International, *CFX-5 Solver and Solver Manager Version 5.6*, CFX-International, 2003.

[7] Raw, M., "Robustness of Coupled Algebraic Multigrid for the (Navier-Stokes) Equations," Tech. Rep. AIAA paper 96-0297, AIAA, 1996.

[8] Barth, T. J. and Jesperson, D. C., "The Design and Application of Upwind Schemes on Unstructured Meshes," Tech. Rep. AIAA paper 89-0366, AIAA, 1989.

[9] Menter, F. R., "Zonal Two-Equation $k - \omega$ Turbulence Models For Aerodynamic Flows," Tech. Rep. AIAA Paper 93-2906, AIAA, 1993.

[10] Bardina, J. E., Huang, P. G., and Coakley, T. J., "Turbulence Modeling Validation, Testing and Development," Tech. Rep. 110446, NASA, 1997.

[11] Collie, S. J., Jackson, P. S., and Gerritsen, M., "Validation of CFD Methods for Downwind Sail Design," *Proceedings of the High Performance Yacht Design Conference*, Auckland, New Zealand, 2002.

[12] ICEM-CFD-Engineering, "ICEM HEXA 4.2," http://www.icemcfd.com/.

[13] Marchaj, C. A., *Aero-Hydro Dynamics of Sailing*, Dodd, Mead & Company, New York, 1979.

[14] Whidden, T. and Levitt, M., *The Art and Science of Sails*, William Collins Sons & Co., Great Britian, 1990.

[15] Cazala, A., "Flow Interaction Between Gennaker and Mainsail," Tech. rep., Department of Mechanical Engineering, University of Auckland, 2002.

[16] Johnson, A. and Stanton, A., "The Flow Interaction of Downwind Sails for America's Cup Class Yachts," Tech. Rep. ME99.25, Department of Mechanical Engineering, The University of Auckland, 1999, Project in Mechanical Engineering Report.

[17] Richards, P. J., Johnson, A., and Stanton, A., "America's Cup Downwind Sails - Vertical Wings or Horizontal Parachutes?" *Journal of Wind Engineering and Industrial Aerodynamics*, Vol. 89, 2001, pp. 1565–1577.